PHYSICAL REVIEW C VOLUME 50, NUMBER 2 AUGUST 1994

Multiple hadron production by 14.5 GeV electron and positron scattering from nuclear targets

P. V. Degtyarenko,* J. Button-Shafer, L. Elouadrhiri, R. A. Miskimen, G. A. Peterson, and K. Wang
Department of Physics and Astronomy, University of Massachusetts, Amherst, Massachusetts 01003

V. B. Gavrilov, M. V. Kossov, G. A. Leksin, and S. M. Shuvalov
Institute of Theoretical and Experimental Physics, Moscow, Russia 117259

F. S. Dietrich, S. O. Melnikoff,† J. D. Molitoris, and K. Van Bibber
Lawrence Livermore National Laboratory, Livermore, California 94550
(Received 20 January 1994; revised manuscript received 28 March 1994)

Multiple proton and pion electroproduction from nuclei are studied. Final states including at least two protons produced by the interaction of 14.5 GeV electrons and positrons with light nuclei (mainly ^{12}C and ^{16}O) have been measured, and compared with analogous data from ^{40}Ar. Scattered electrons and positrons were detected in the energy transfer range from 0.2 to 12.5 GeV, and four-momentum transfer squared range from 0.1 to 5.0 GeV$^2/c^2$. Phenomenological characteristics of the secondary hadron production cross sections such as temperature and velocity of the effective source of hadrons were found to be dependent on energy transfer to the nucleus and independent on the four-momentum transfer squared at energy transfers greater than 2 GeV.

PACS number(s): 25.30.Fj, 25.30.Rw, 13.60.Le

The understanding of highly excited nuclear matter presents a challenge to strong interaction physics [1]. Particle production off nuclei in a kinematical region which is forbidden for reactions on quasifree nucleons [2], the EMC effect [3], and other experimental evidence indicate that for certain conditions nuclei may not be considered as groups of quasifree nucleons, and/or that the properties of nucleons inside nuclei, such as their structure functions, are different from those of free nucleons. Theoretical approaches to understand these effects based upon QCD seem to be difficult, but phenomenological models using multiquark bags, droplets of quark-gluon plasma, or projectile interactions with closely correlated groups of nucleons [4], are available. Experiments at energies above approximately 1 GeV show several regularities [2]. These include the lack of dependence of secondary particle spectra on projectile energy and type, atomic number of the target nucleus, the saturation of yields of the secondary particles from nuclei at some critical incident energy varying approximately as $A^{1/3}$ ("limiting nuclear fragmentation"), and other effects known also as "nuclear scaling" phenomena. These experimental regularities can be described by a scenario called "deep inelastic nuclear reaction" (DIN) [2], for which the first stage is the interaction of the projectile with the nucleus, transferring part of its energy and momentum and causing a local excitation inside the nucleus. The second stage is the cooling of the excitation by means of nucleon emission and meson production. The energy transfer mechanism may be different for different types of projectiles; the common feature is limited energy that might be absorbed by the nucleus.

In order to clarify the situation phenomenologically, new experiments using large acceptance detectors and electron beams are highly desirable. The measurement of the nuclear response to the electron's pointlike excitation may help in the analysis of more complicated interaction processes such as hadron-nucleus or nucleus-nucleus collisions. As a first attempt to implement this strategy, we have analyzed electron-nucleus interaction data taken at 14.5 GeV with the TPC/2γ detector [5] at the PEP electron-positron storage ring at SLAC. This detector has large acceptance, large kinematic coverage in four-momentum transfer squared Q^2 and in energy transfer ν, and the ability to detect many-body final states.

The detector has been described in detail elsewhere [6,7]. The Time-Projection Chamber (TPC) tracks particles in a 13.25 kG solenoidal magnetic field, using momentum and dE/dx measurement for particle identification, as shown in Fig. 1 for our results. The solid angle coverage is approximately 90% of 4π sr. Positrons and electrons scattered at small angles (θ_e from 22 to 180 mr) were tagged in the forward "2γ" spectrometers located at each end of the TPC. The scattering resulted from the e^+ or e^- interacting with the nuclei of residual gas (H_2 and CO) in the PEP ring vacuum chamber, and also with injected argon gas in dedicated runs [8]. For the analysis reported here the detector trigger was required to have at least one charged hadron in the TPC and an e^+ or e^- tag with energy greater than 2 GeV in one of the forward spectrometers. The selection of nuclear interactions required at least two tracks in the TPC with a common vertex at least 5 cm, but no more than 25 cm along the beam line from the e^+e^- interaction region. Additional procedures to the standard TPC data processing were performed, such as determination of the vertex position far from the e^+e^- interaction point and corrections of electron scattering variables using new vertex information. To eliminate

*On leave from Institute of Theoretical and Experimental Physics, Moscow, Russia 117259.

†Present address: 11 Surf Way, Novato, CA 94945-1741.

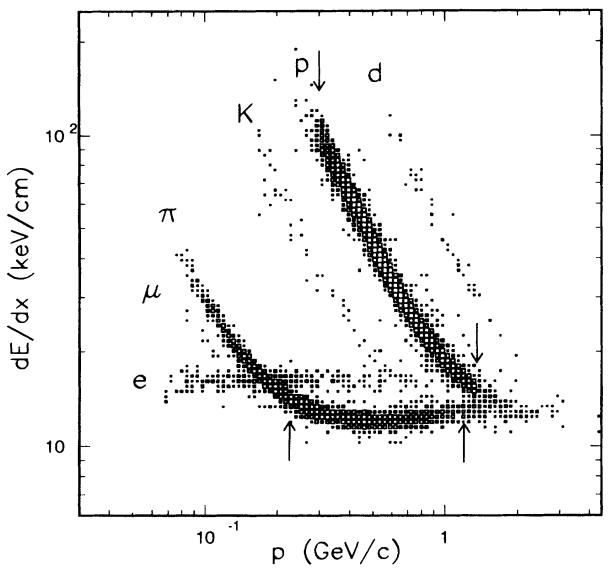

FIG. 1. Particle identification by specific energy deposition dE/dx for the TPC detector vs p, where p is the momentum of the particle. The size of the square plotted at each bin is proportional to the logarithm of the number of entries in the bin. Arrows show the limits on momentum used to identify unambiguously protons and charged pions.

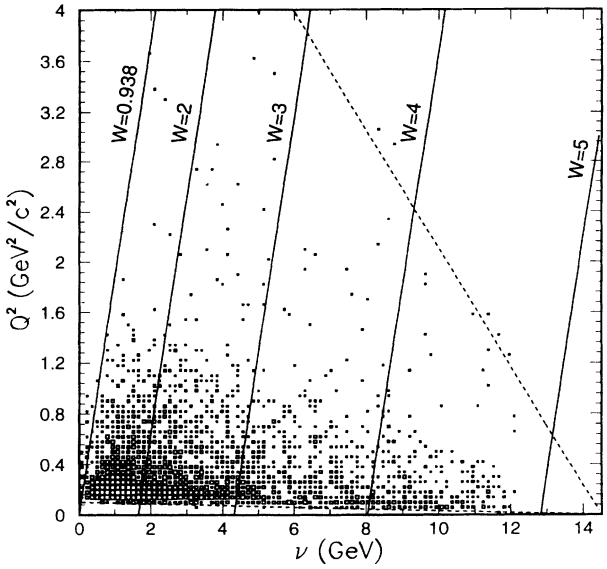

FIG. 2. Experimental distribution of the events on Q^2 vs ν plot. The size of the square plotted at each bin is proportional to the logarithm of the number of entries in the bin. The dashed lines correspond to the limits of the polar scattering angle of the electron, θ_e = 22 and 180 mr. The solid lines show the set of W intervals.

interactions on H_2 and to suppress e^+e^- interactions in the data sample, we accepted events with the number of identified protons greater than or equal to two. Then the selected events are of the type

$$(e^+, \text{ or } e^-)+A \rightarrow e'+p+p+\text{anything}, \qquad (1)$$

where A represents either $^{12}C+^{16}O$ or ^{40}Ar. This selection cuts off part of the events characteristic for DIN reactions, namely events with a single proton emitted in the backward hemisphere in the laboratory frame. But apart from the methodical advantages of using reaction type (1), we acquire the possibility of performing angular and momentum analysis in the full solid angle. The fraction of backward proton tracks not included in the analysis is $\approx$ 40% for (CO) and $\approx$ 30% for Ar targets. The number of events of reaction (1) selected for analysis was 2979 and 316 for CO and Ar targets, respectively. Rough estimates based upon data from high energy hadron-induced reactions [2], and the similarity of the characteristics of the secondary hadrons in multihadron production, indicate that the class of events of the reaction type (1) may represent, for comparable energy and momentum transfers, up to 10–25 % of the total inelastic cross section for light nuclei, such as C and O, and up to 20–50 % for heavy nuclei.

In our analysis we denote the incident and final electron four momentum as $k_0=(E_0,\mathbf{k}_0)$ and $k'=(E',\mathbf{k}')$; the four-momentum transfer is $q=k_0-k'\equiv(E_0-E',\mathbf{q})\equiv(\nu,\mathbf{q})$; $Q^2=-q^2$; the effective mass of the recoil system W (provided that the electron interacts with a nucleon at rest) is $W^2=M_N^2+2M_N\nu-Q^2$, where M_N is the nucleon mass.

In Fig. 2, the experimental distribution of the events on a Q^2 versus ν plot shows a maximum at low Q^2 (0.2 GeV$^2/c^2$) and relatively low ν (1 GeV). The dashed lines show acceptance limits of the "2γ" electron detectors, according to the relation $Q^2=4E_0(E_0-\nu)\sin^2(\theta_e/2)$. The solid lines represent the series of W values.

We shall characterize the nuclear response in terms of one-particle inclusive distributions for the hadrons in the events of type (1) normalized by the total number of events of type (1) n_{reaction}, i.e., the measured "differential multiplicity" $\rho^*=n^*_{\text{incl}}/n_{\text{reaction}}$, where

$$n_{\text{incl}} = \frac{Ed^3n}{d\mathbf{p}^3} \equiv \frac{d^2n}{2\pi p\, dT\, d\cos\Theta}. \qquad (2)$$

We denote the four momentum of the secondary hadron as $(E,\mathbf{p})$, and its kinetic energy in laboratory system as T. The polar angle Θ of its emission in the laboratory system is taken relative to the direction of the three momentum transferred to the nucleus $\mathbf{q}$, chosen to be the direction of the z axis in the reaction. The (*) denotes measurement of one-particle differential multiplicities for the e-A interactions of type (1) with the electron scattered within the acceptance of the detector (θ_e=22–180 mr), and with at least two protons with momenta 0.3–1.5 GeV/c in the event.

Acceptance corrections were calculated for each experimental point (interval in electron variables, e.g., ν and Q^2, and interval in secondary particle variables, e.g., T and $\cos\Theta$) as the ratio of the number of Monte Carlo events which passed all trigger and selection criteria determined by the detector simulation routine to the number of Monte Carlo generated events which give entries to this interval. The computer program GLOBAL [7] has been used to simulate the trigger and detector response, including resolution effects, energy loss, multiple scattering, and nuclear interactions in the detector materials. Apart from the acceptance and effi-

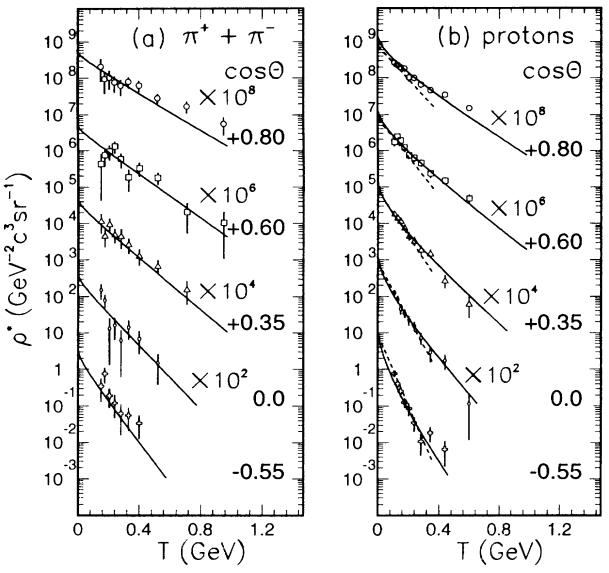

FIG. 3. (a) Charged pion and (b) proton production in e-(CO) interactions. The function of differential multiplicity $\rho^*(T,\cos\Theta)$ is shown as a series of spectra in laboratory kinetic energy T. The spectra are binned in five $\cos\Theta$ intervals for $-0.9<\cos\Theta<0.9$, with midinterval values shown. The spectra are displaced vertically by multiplying each by powers of 100 for each $\cos\Theta$ interval. Dashed lines represent parametrization of the spectra taken from Ref. [11]. Solid lines correspond to Eq. (4) with fitted parameter values.

ciency corrections of the "2γ" detectors which measured scattered electrons, the acceptance corrections for the hadrons were determined by the TPC efficiency, which is smooth to within $\sim 20\%$ in the range of momenta under consideration, and by the angular acceptance of the TPC, which has practically zero forward and backward efficiencies for $|\cos\Theta_{\rm lab}|>0.9$ in the laboratory frame. In general, as the direction of the transferred momentum in the reaction $A(e,e')\ldots$ is not coincident with the z direction in the laboratory frame, these corrections were essential for $|\cos\Theta|>0.75$ and were also of the order of 20%. The DINREG event generator [9] used as the input for the acceptance calculation has been tuned up to reproduce distributions on ν and Q^2 for electrons, multiplicity of protons and pions in the reaction, and the angular and momentum spectra of the secondary protons and pions. To estimate the sensitivity of the results to the choice of the input event generator, the acceptance correction calculation has also been performed by using the VENUS3 event generator [10].

To illustrate the procedure of the analysis, the kinetic energy spectra of charged pions $\rho^*_\pi(T)=\rho^*_{\pi^+}+\rho^*_{\pi^-}$ and protons $\rho^*_p(T)$ coming from CO measured in five intervals of $\cos\Theta$, in the range of $1.7<\nu<2.9$ GeV, are shown in Fig. 3. The spectra show well-known exponential behavior with the slopes increasing as Θ increases. The dashed lines in the figure show a parametrized approximation of the inclusive proton spectra in the pion-induced DIN reaction $\pi+C\rightarrow p+$anything at 5 GeV/c [11]. The series is normalized to the data at $\cos\Theta=0$. Our data are quite close to the parametrization in the comparable region of the energy transfer to the nucleus and for proton kinetic energy range 0.08–0.3 GeV, corresponding to the energy range of Ref. [11].

In order to investigate the dependence of the nuclear response on the four-momentum transfer to the nucleus, we tried to find a minimal set of parameters describing the proton and pion spectra. We have found that a parametrization similar to the one first used in the thermodynamic quark-parton model of multiple hadron production on nuclei [12] can satisfactorily approximate the proton and pion spectra ($\chi^2/N\lesssim 1.7$), with four parameters dependent on the mean ν of the reaction. The phenomenological basis for the model is the scenario of DIN reactions [2], which was developed using several assumptions related to electron-nucleus scattering. The first assumption is that the object inside the nucleus that locally absorbs transferred four momentum is a nucleon or group of nucleons at rest or smeared with Fermi motion. The excited source is assumed to be composed of quark partons moving isotropically in the source rest frame and distributed exponentially in energy k:

$$f_{\rm inv}=\frac{dN}{k\,dk}=\text{const}\,\exp(-k/t), \tag{3}$$

where $f_{\rm inv}$ is the invariant phase-space density, and t is a parameter representing characteristic temperature. The excitation cools off by the emission of pions from the excited source and by the interaction of the excited source with the nucleons in the residual nucleus. A quark from the source is exchanged with a quark of the same color from one of these nucleons to form a nucleon in the final state. Energy and momentum conservation in the exchange process leads to the kinematical link between the momentum of the secondary hadron and k: $k=(p_p+T_p)/2$ for protons and $k=(p_\pi+E_\pi)/2$ for pions in the laboratory frame. A Lorentz transformation of the exponential distribution of the quarks in the source (3) to the laboratory frame gives $\rho_i=C_i\exp[-k\gamma(1-v\cos\Theta)/t]$, where i stands for secondary proton or pion, C_i is a normalization parameter, v is the velocity of the source, $\gamma=(1-v^2)^{-1/2}$, and if we use the parameter $\delta=\gamma v$, then

$$\rho_i=C_i\exp[-k(\sqrt{1+\delta^2}-\delta\cos\Theta)/t]. \tag{4}$$

The solid lines in Fig. 3 are the result of the fit of the data using Eq. (4). The values of t and δ parameters and χ^2/N as a function of ν interval are given in the upper portion of Table I for (CO) and Ar targets. The temperature parameter t saturates as ν increases; the saturated temperature is the same within errors for CO and Ar. It is also close to the value deduced from the analysis of p-A interactions at much higher energy (400 GeV): $t_{pA}=0.140$ GeV from Ref. [12]. The $\delta(\nu)$ dependence shows a slow increase for CO as ν increases and is lower for Ar.

The parametrization of the spectra for CO made in three Q^2 intervals in the $W>2$ GeV region beyond resonance electron scattering is also given in Table I. Within errors we do not observe changes in the parameters as Q^2 is increased from approximately 0.1 to 1.5 GeV$^2/c^2$.

The systematical difference of the parameters characterizing the shapes of the spectra, t and δ, obtained by using the two different input event generators for the acceptance cor-

TABLE I. Parameter values deduced from fitting secondary proton and pion spectra with Eq. (4). The one-standard-deviation statistical uncertainties are shown within parentheses.

					C_i ($GeV^{-2}c^3sr^{-1}$)		χ^2/N	
Target	ν (GeV)	t (GeV)	δ	C_π/C_p	protons	pions	protons	pions
CO	0.2–0.6	0.053(0.003)	0.23(0.03)	···(···)	309(42)	···(···)	0.55	···
(all Q^2)	0.6–1.1	0.084(0.003)	0.41(0.03)	0.15(0.05)	39.4(3.2)	6.1(1.9)	1.57	0.18
	1.1–1.7	0.112(0.004)	0.54(0.04)	0.27(0.05)	18.0(1.2)	4.9(0.9)	0.84	0.61
	1.7–2.9	0.118(0.004)	0.60(0.03)	0.50(0.05)	16.5(0.9)	8.2(0.8)	0.95	0.94
	2.9–4.5	0.126(0.005)	0.70(0.05)	0.98(0.08)	11.9(0.8)	11.7(1.0)	1.52	0.82
	4.5–6.1	0.125(0.008)	0.81(0.08)	1.41(0.14)	10.7(0.9)	15.0(1.6)	1.46	1.21
	6.1–8.1	0.132(0.009)	0.80(0.07)	1.22(0.15)	8.5(0.8)	10.4(1.3)	0.98	0.92
	8.1–12.0	0.146(0.014)	0.98(0.10)	1.79(0.20)	5.6(0.5)	10.0(1.1)	1.79	0.76
^{40}Ar	0.2–1.7	0.103(0.012)	0.44(0.08)	0.60(0.33)	15.8(2.6)	9.4(5.2)	0.71	0.14
(all Q^2)	1.7–4.5	0.139(0.011)	0.61(0.10)	0.77(0.15)	10.4(1.3)	8.0(1.6)	1.17	0.36
	4.5–12.0	0.120(0.010)	0.52(0.08)	0.93(0.15)	19.2(2.5)	17.9(3.0)	0.52	0.57
	Q^2 (GeV^2/c^2)							
CO	0.1–0.4	0.125(0.003)	0.66(0.03)	0.97(0.05)	12.4(0.5)	12.0(0.7)	1.76	1.44
($W>2$)	0.4–0.8	0.124(0.006)	0.70(0.06)	1.02(0.10)	12.4(1.0)	12.6(1.3)	1.36	0.82
	0.8–5.0	0.116(0.008)	0.66(0.09)	0.98(0.14)	12.8(1.4)	12.5(1.9)	0.95	0.75

rection calculations mentioned above, was found on average to be less than 10% for t and 5% for δ, to not exceed 15% in different intervals of W and Q^2, and to not exceed 5% in point-to-point systematics. The normalization parameters proved to be more sensitive to the choice of the input event generator for the acceptance calculations. The C_π/C_p ratio shows a systematic shift of about 30% for all points while keeping the functional dependence on W and independence of Q^2 the same.

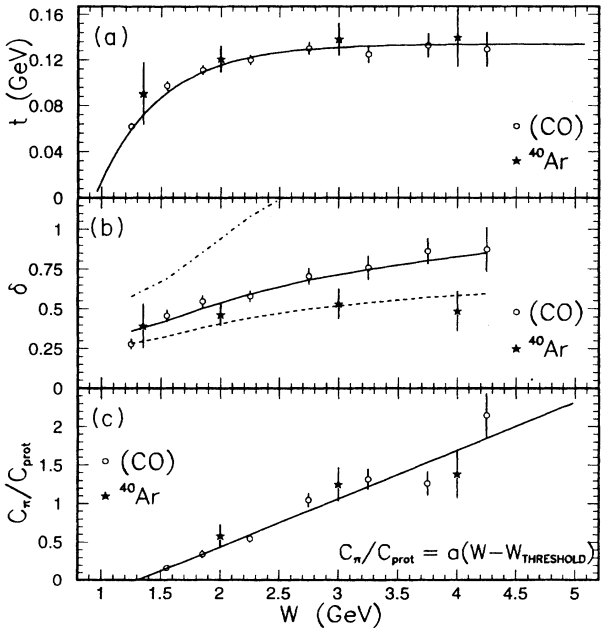

FIG. 4. The W dependence of the parameters (a) t, (b) δ, and (c) the ratio C_π/C_p. The values of the parameters are deduced from the fitting of the secondary proton and pion spectra with Eq. (4). See details in the text.

Radiative corrections were not calculated because they require iteration procedures which are impossible at the statistical level of this experiment. The thickness of equivalent radiators [13] which should be put before and after the scattering vertex to take into account the bremsstrahlung processes on the nucleus is estimated to be 2–5 % of a radiation length for CO, and 2–10 % for Ar targets in the Q^2 and ν ranges under consideration. This value roughly characterizes the effective systematic shift in ν: $d\nu/\nu$ is increased from about 2% at low $\nu \approx 0.5$ GeV to about 5% (CO) and about 10% (Ar) at high $\nu \approx 10$ GeV. We also believe it is small enough to make the effects of smearing of the chosen wide Q^2 and ν intervals small within the statistical errors. These effects may be taken into account exactly in model calculations.

The events are concentrated at low Q^2, so the variables ν and W are closely correlated, as one may see in Fig. 2, especially in the region of high $\nu>2$ GeV, or $W>2$ GeV. Within the framework of the phenomenological model used for the parametrization of the spectra, the value of $W-M_N$ may be used as a measure of the excitation of a nucleon inside nucleus; the considerations are similar in the case of nucleon clusters. Figures 4(a) and 4(b) show the dependences of t and δ parameters on W, and Fig. 4(c) shows the W dependence of the pion to proton ratio of the normalization parameters C_π/C_p.

The $t(W)$ saturation at high excitations may be qualitatively understood within the concept of finite or limited Hagedorn temperature of the excited source [14]. At small excitations the influence of the kinematical limits and four-momentum conservation must lead to an effective decrease of the temperature parameter. Empirically, we could try to derive a parametrization of the $t(W)$ dependence assuming that the energy transferred to the nucleon takes the form of additional $q\bar{q}$ pairs produced in the excited source. If the quark spectrum is defined by Eq. (3), then the mean energy

in the source rest frame of one massless quark is $\int k^2 \exp(-k/t)dk/\int k \exp(-k/t)dk = 2t$. At low excitations one should consider only one $q\bar{q}$ pair, hence $t=(W-M_N)/4$ at small values of $W-M_N$. With increasing $W-M_N$ the probability to produce more than one pair should be taken into account. Now if we postulate the existence of the Hagedorn temperature t_0, then in the limit of very large $W-M_N$ we should have $t(W)=\text{const}=t_0$. As an approximation between these two boundary conditions we may write the function

$$t(W)=t_0\{1-\exp[-(W-M_N)/(4t_0)]\}. \quad (5)$$

The solid line in Fig. 4(a) shows $t(W)$ dependence defined by Eq. (5) with the fitted value of the parameter $t_0=0.134\pm0.003$ GeV.

One may obtain a phenomenological understanding of the $\delta(W)$ dependences presented in Fig. 4(b) by considering the kinematics of the excited source. Suppose the virtual photon transfers 100% of its energy and momentum to a nucleon without momentum being transferred to the residual nucleus. The $\delta(W)$ dependence calculated for such a case is represented by the dash-dotted line in Fig. 4(b), and is much higher than the data. This may indicate that a fraction of the transferred momentum $\varepsilon\mathbf{q}$ is transferred to the residual nucleus resulting in the slowing down of the excited source. The CO data may be approximated by a $\delta(W)$ calculated with $\varepsilon=0.31$ [solid line in Fig. 4(b)], and the Ar data with $\varepsilon=0.45$ (dashed line). The difference between ε for CO and Ar may be roughly attributed to the difference of mean paths of the source inside the nuclei. The excitation of heavier nucleon clusters in the nucleus may also play a role in the observed $\delta(W)$ dependence.

The C_π/C_p ratio in Fig. 4(c) is increasing linearly as a function of W: $C_\pi/C_p=a(W-W_{\text{threshold}})$ with $a=0.63\pm0.04$ and $W_{\text{threshold}}=1.31\pm0.07$ GeV. This effect may be understood within the framework of the model under consideration: the higher the excitation, the higher the portion of the source phase space available for pion production. Quantitative understanding of the parameters a and $W_{\text{threshold}}$ may not be so obvious because they might be connected with the trigger and selection criteria used to separate the reaction type (1). The coincidence within errors of the C_π/C_p ratios for (CO) and Ar targets [Fig. 4(c)] may be considered as additional evidence in favor of "nuclear scaling" phenomena.

In conclusion, we have measured one-particle differential multiplicities of secondary protons and charged pions in electronuclear reactions of type (1) at 14.5 GeV. Outside the resonance region of electron scattering we do not observe any Q^2 dependence of the nuclear fragmentation down to 0.1 GeV^2. We observe clear dependence of the characteristics of the secondary hadron production on ν and W which may be treated in terms of the phenomenological parameters of a characteristic temperature and velocity of an excited source.

This paper presents a possible phenomenological approach to understanding the data. We expect more specific and detailed comparisons with theoretical models in future publications.

We thank the members of the SLAC TPC/2γ Collaboration, in particular, R. Belcinski, A. M. Eisner, K. H. Fairfield, R. R. Kofler, and G. R. Lynch, for their able assistance. This work was supported in part by the U.S. Department of Energy through Grant No. DE-FG02-88ER40415, by Lawrence Livermore National Laboratory through Contract No. W-7405-ENG-48, and by NSF Grant No. HRD-9103574.

[1] S. J. Brodsky, Nucl. Phys. **A544**, 223 (1992).
[2] V. B. Gavrilov, G. A. Leksin, S. M. Shuvalov, and K. Sh. Egiyan, Nucl. Phys. **A532**, 321 (1991).
[3] J. J. Aubert *et al.*, Phys. Lett. **123B**, 275 (1983).
[4] L. Frankfurt and M. Strikman, Phys. Rep. **160**, 235 (1988).
[5] J. N. Marx and D. R. Nygren, Phys. Today **31** (10), 46 (1978); H. Aihara *et al.*, Report No. LBL-23737, 1988.
[6] M. P. Cain *et al.*, Phys. Lett. **147B**, 232 (1984).
[7] A. R. Barker, Ph.D. thesis, University of California, Santa Barbara, 1988.
[8] S. O. Melnikoff, in *Proceedings of the Workshop on Electronuclear Physics with Internal Targets*, Stanford, 1987, edited by R. G. Arnold and R. C. Minehart, Report No. SLAC-316.
[9] P. V. Degtyarenko and M. V. Kossov, Report No. ITEP 11-92, Moscow, 1992.
[10] K. Werner and P. Koch, Z. Phys. C **47**, 255 (1990).
[11] Yu. D. Bayukov *et al.*, Sov. J. Nucl. Phys. **42**, 116 (1985).
[12] M. V. Kossov and L. M. Voronina, Report No. ITEP 165-84, Moscow, 1984.
[13] L. W. Mo and Y. S. Tsai, Rev. Mod. Phys. **41**, 205 (1969).
[14] R. Hagedorn and J. Rafelski, Phys. Lett. **97B**, 136 (1980).